List of Supplementary figures:

Figure S1: A example of offline radiative transfer calculation showing the effect of BBA on Irradiances. This was calculated using the SOCRATES radiative transfer model. 3

Figure S2: Showing the Gross primary productivity against the total PAR binned by diffuse fraction (top) and Gross primary productivity against diffuse fraction binned by Total PAR (bottom) based on simulations from the JULES model (a and b) and the HadGEM2-ES model (c and d). 4

Figure S3: Time series of GPP (a), Plant Respiration (b) and Net Primary Productivity (c) for the French Guyana site as simulated by the JULES model for varying Leaf nitrogen concentration at canopy top. Corresponfing annual mean of GPP (d), Plant Respiration (e) and Net Primary Productivity (f) against Leaf nitrogen concentration at canopy top. 5

Figure S4: Showing on a), the annual mean of NPP (filled contour), GPP (red iso-contours) and Plant Respiration (black dashed iso-contours) against dark respiration coefficient (X-axis) and Leaf nitrogen concentration at canopy top (Y-axis). Showing on b), the same quantities as a) but plotted against the nitrogen extinction coefficient (see text, X-axis) and mean canopy carboxylation rate (Vcmax,25, Y-axis). Showing on c) the corresponding leaf nitrogen concentration at canopy top for a given combination of the mean canopy carboxylation rate and the nitrogen extinction coefficient. On a), a nitrogen extinction coefficient of 0.156 was assumed, while on b) and c) a dark respiration coefficient of 15% was assumed. 6

Figure S5: The tile fraction covered by broadleaf tree (a) and C3 grass (b). 7

Figure S6: The modelled seasonal cycle of biomass burning aerosol SSA (a) and total aerosol SSA (b), for the BBAx1 run for different BBA absorption assumption (ABS is for more absorbing, DIF is for more scattering)). Impact of varying BBA optical properties on the surface PAR fluxes (c). 8

Figure S7: A simplified schematic showing some of the pathways of interaction between Biomass Burning and vegetated land surface. 9

Figure S8: Multi-year mean Seasonal cycle averaged over central Amazon defined by the coordinates EQ-15°S / 70°W-53°W, for the (a) GPP, (b) NPP, (c) surface precipitation, (d) surface temperature (c), (e) full sky (f) and clear-sky short wave surface radiation. Seasonal cycle for HadGEM2-ES BBAx1 simulation is shown in black, while seasonal cycles derived from observational dataset are shown in blue. Observational dataset/proxy are taken from FLUXCOM (a), MODIS 17A2 (b), CRU (c and d) and CERES (e and f). .. 10

Figure S9: Mean seasonal cycle of GPP anomalies (a), Plant Respiration, R_p, anomalies (b) and NPP anomalies (c) for the varying BBA emission scenarios (see text, section 2.2) averaged over the Amazon basin defined by the coordinates EQ-15°S / 70°W-53°W. Differences are calculated with regards to experiment BBAx0 and represented by the plain curves (left axis). The short-dash curves correspond to the accumulated anomalies (right y-axis). Note the reduced scales on the y-axis on b). 11

Figure S10: Showing the 30-year mean from the BBAx1 simulation of the (grid box?) cloud optical thickness (a,b) and the total cloud fraction (c,d) for August (left) and September (right). 12

Figure S11: Showing changes in a) Soil moisture availability, b) vegetation evapotranspiration, c) evaporative fraction and d) Water Use Efficiency for the varying BBA emissions scenarios averaged over the domain of analysis defined by the coordinates EQ-15°S / 70°W-53°W (see text). 13

Figure S12: Canopy temperature (first row), Vapour Pressure Deficit (VPD, second row) and Rate of carboxylation of the Rubisco enzyme ($V_{c,max}$) normalised by the maximum rate at 25°C ($V_{c,max,25}$, third row) for the reference simulation (BBAx0, a, e, i) and for the simulations that include BBA emissions (respectively, BBAx1, b,f,j; BBAx2, c,g,k and BBAx4, d,h,l). VPD and $V_{c,max}$ are calculated using the Collatz et al. (1991, 1992) C3 model and assuming the plant functional type traits of broadleaf trees from HadGEM2-ES (Clark et al., 2011). Calculations are done 'a posteriori' (i.e. offline) using the radiation and the meteorological variables derived from the 3h history of HadGEM2-ES instantaneous outputs of the first 8 years of simulation which are sampled over the domain of analysis during daytime when the surface total radiation is superior to 100 W/m^2. As $V_{c,max}$ is solely a function of leaf temperature, we have represented the theoretical curve (in grey). The size of the circles in the bottom plots represent the frequency of occurrence of a given temperature value in the dataset sampled over the domain of analysis defined by the coordinates EQ-15°S / 70°W-53°W..... 14

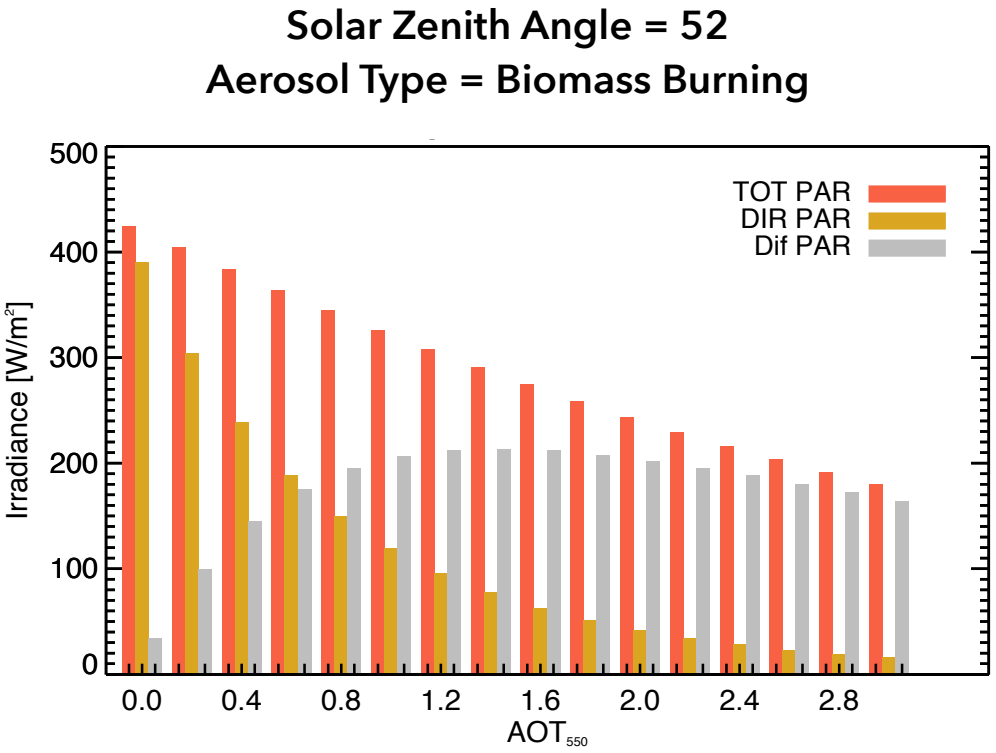

Figure S1: A example of offline radiative transfer calculation showing the effect of BBA on Irradiances. This was calculated using the SOCRATES radiative transfer model.

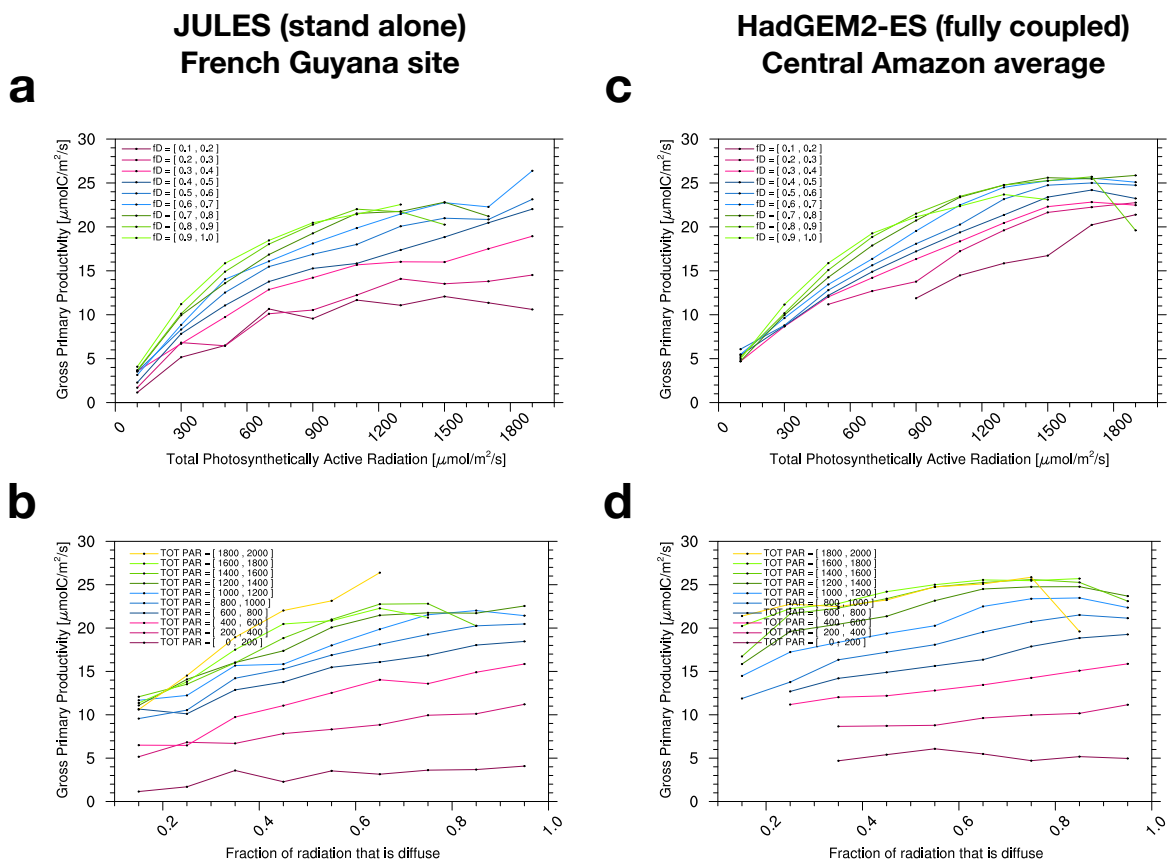

Figure S2: Showing the Gross primary productivity against the total PAR binned by diffuse fraction (top) and Gross primary productivity against diffuse fraction binned by Total PAR (bottom) based on simulations from the JULES model (a and b) and the HadGEM2-ES model (c and d).

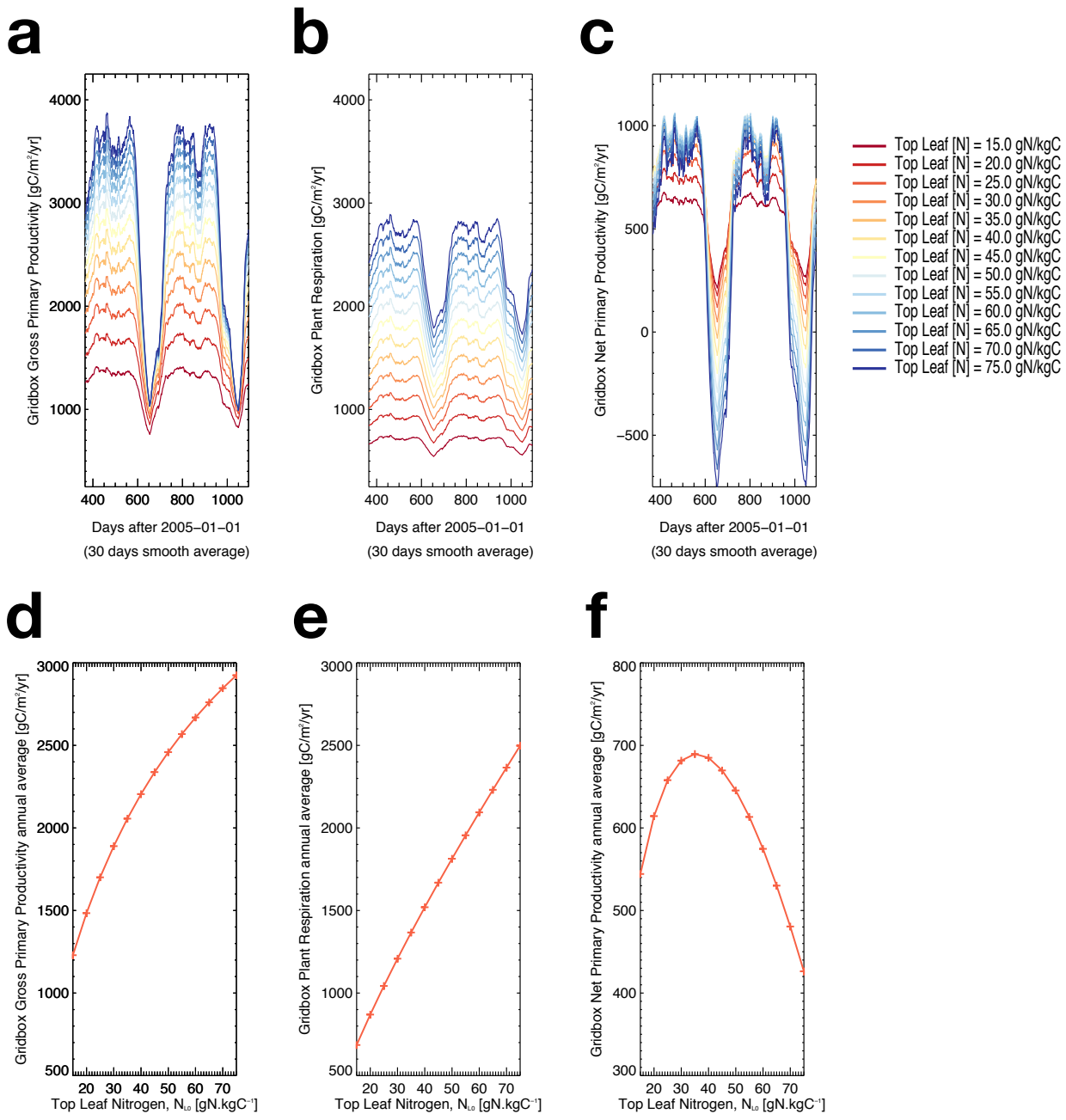

Figure S3: Time series of GPP (a), Plant Respiration (b) and Net Primary Productivity (c) for the French Guyana site as simulated by the JULES model for varying Leaf nitrogen concentration at canopy top. Corresponfing annual mean of GPP (d), Plant Respiration (e) and Net Primary Productivity (f) against Leaf nitrogen concentration at canopy top.

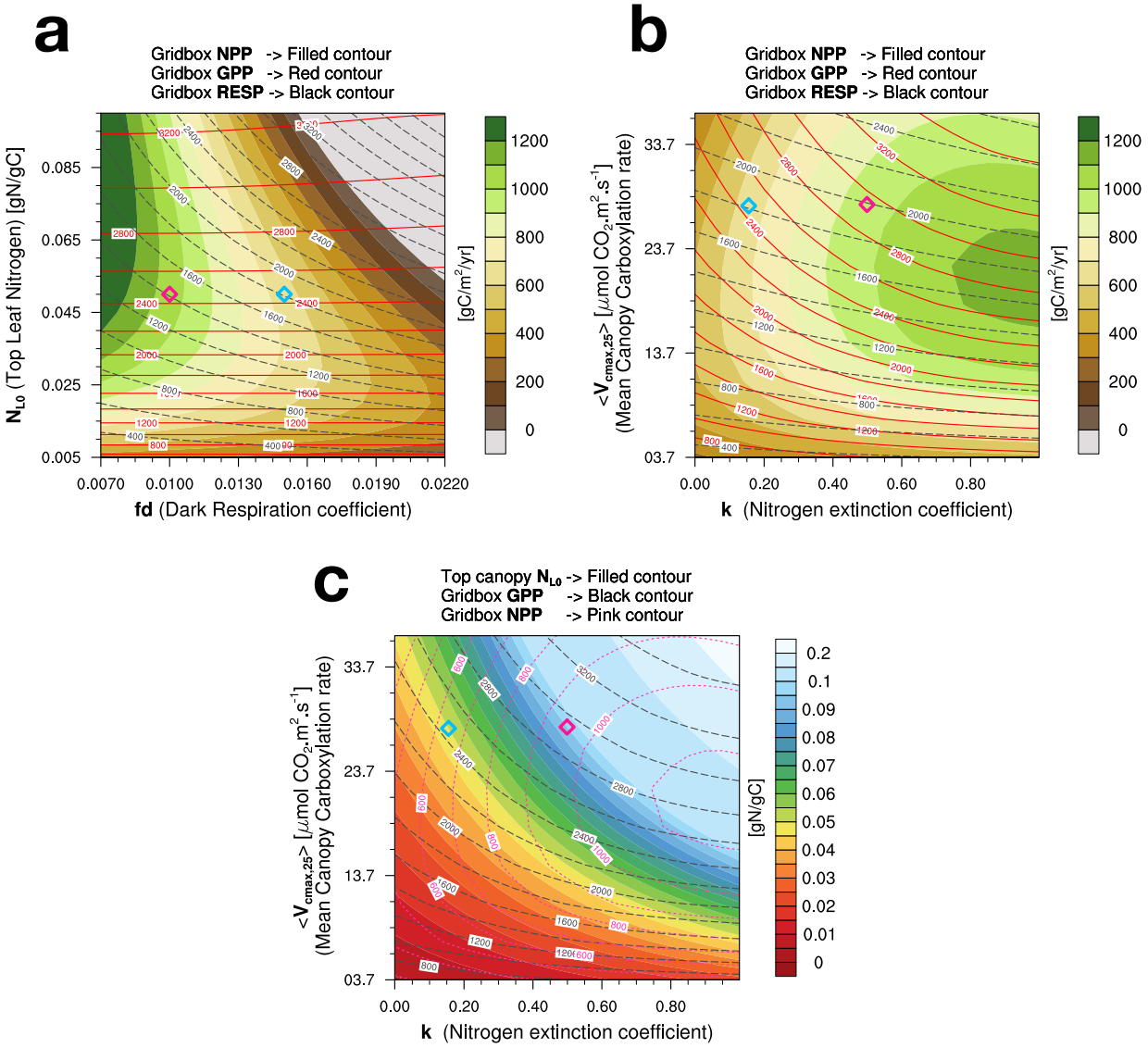

Figure S4: Showing on a), the annual mean of NPP (filled contour), GPP (red iso-contours) and Plant Respiration (black dashed iso-contours) against dark respiration coefficient (X-axis) and Leaf nitrogen concentration at canopy top (Y-axis). Showing on b), the same quantities as a) but plotted against the nitrogen extinction coefficient (see text, X-axis) and mean canopy carboxylation rate ($V_{cmax,25}$, Y-axis). Showing on c) the corresponding leaf nitrogen concentration at canopy top for a given combination of the mean canopy carboxylation rate and the nitrogen extinction coefficient. On a), a nitrogen extinction coefficient of 0.156 was assumed, while on b) and c) a dark respiration coefficient of 15% was assumed.

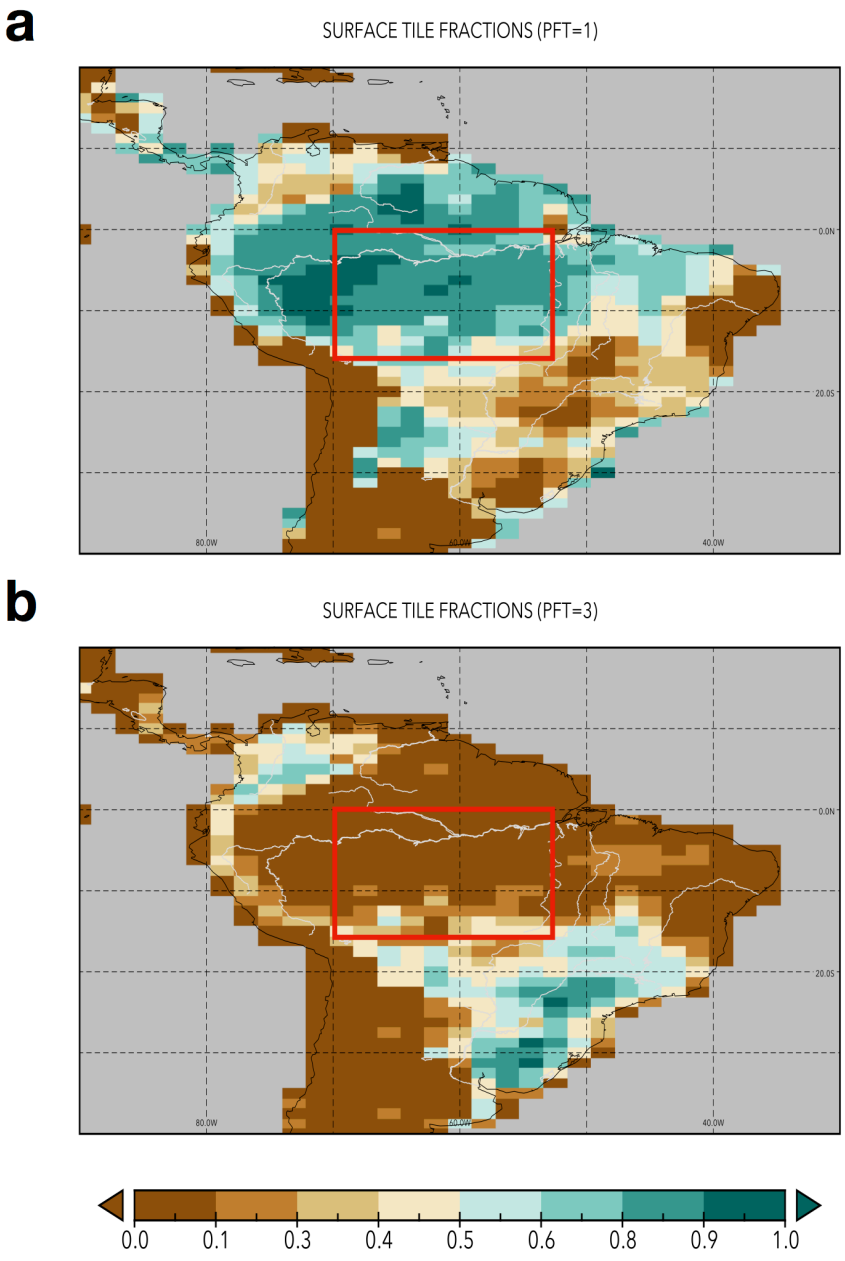

Figure S5: The tile fraction covered by broadleaf tree (a) and C3 grass (b).

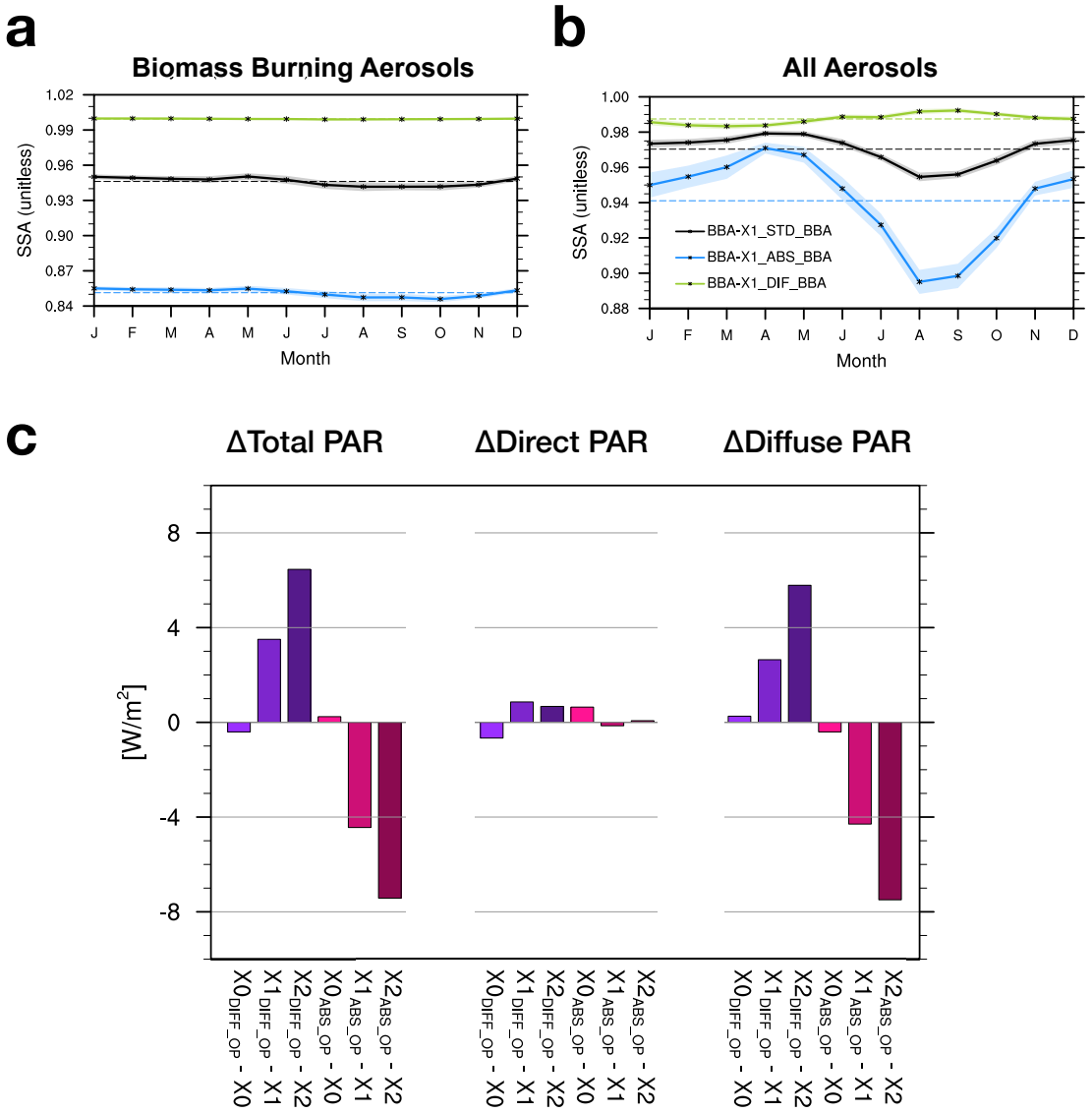

Figure S6: The modelled seasonal cycle of biomass burning aerosol SSA (a) and total aerosol SSA (b), for the BBAx1 run for different BBA absorption assumption (ABS is for more absorbing, DIFF is for more scattering)). Impact of varying BBA optical properties on the surface PAR fluxes (c).

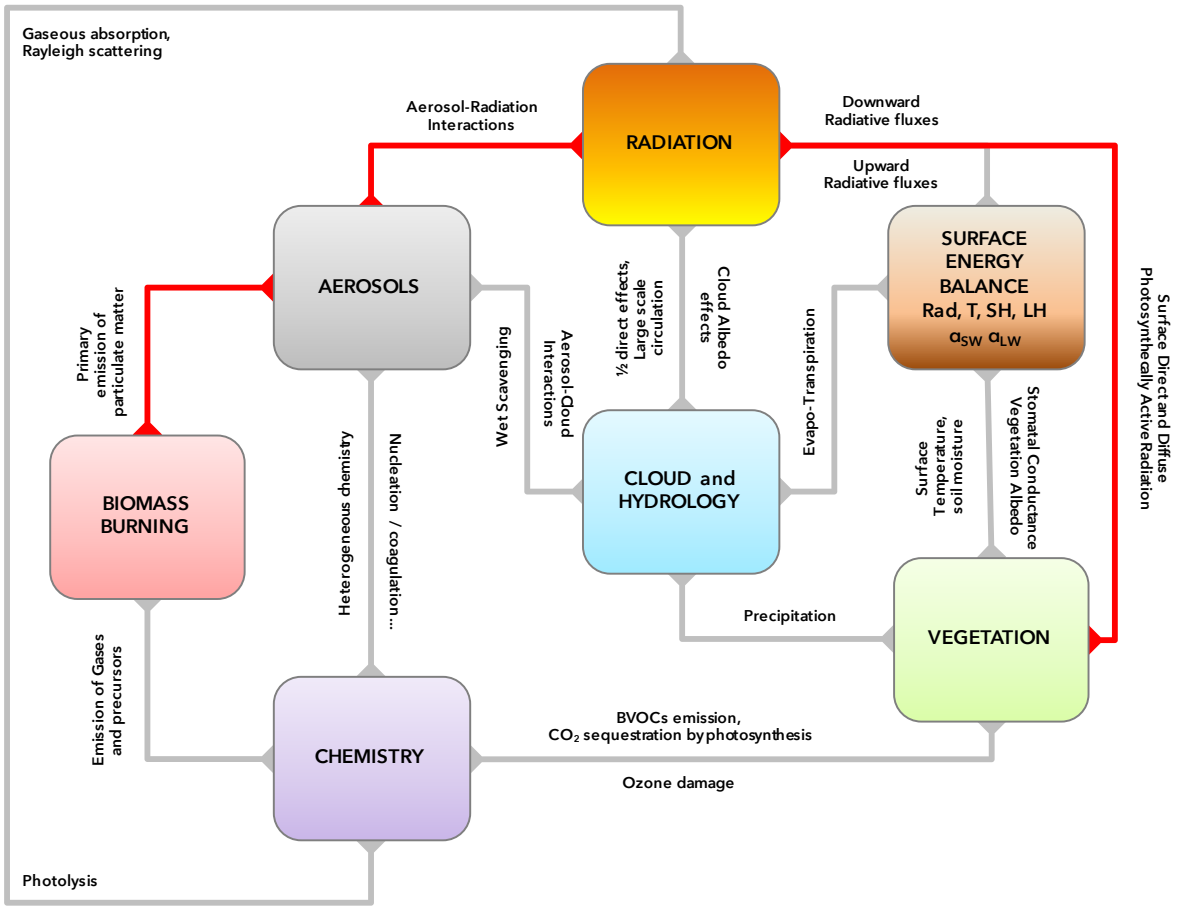

Figure S7: A simplified schematic showing some of the pathways of interaction between Biomass Burning and vegetated land surface.

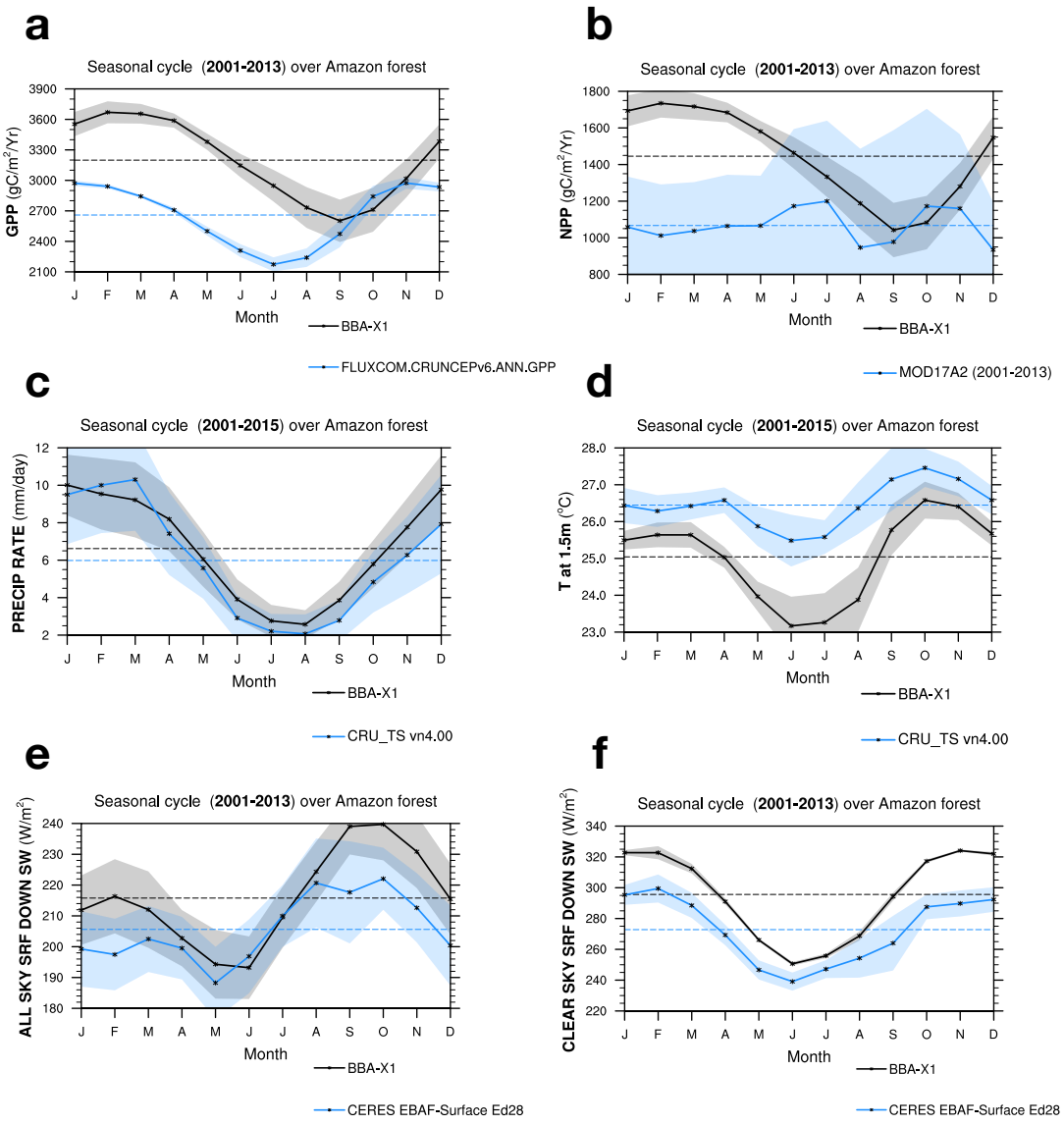

Figure S8: Multi-year mean Seasonal cycle averaged over central Amazon defined by the coordinates EQ-15°S / 70°W-53°W, for the (a) GPP, (b) NPP, (c) surface precipitation, (d) surface temperature (c), (e) full sky (f) and clear-sky short wave surface radiation. Seasonal cycle for HadGEM2-ES BBAx1 simulation is shown in black, while seasonal cycles derived from observational dataset are shown in blue. Observational dataset/proxy are taken from FLUXCOM (a), MODIS 17A2 (b), CRU (c and d) and CERES (e and f).

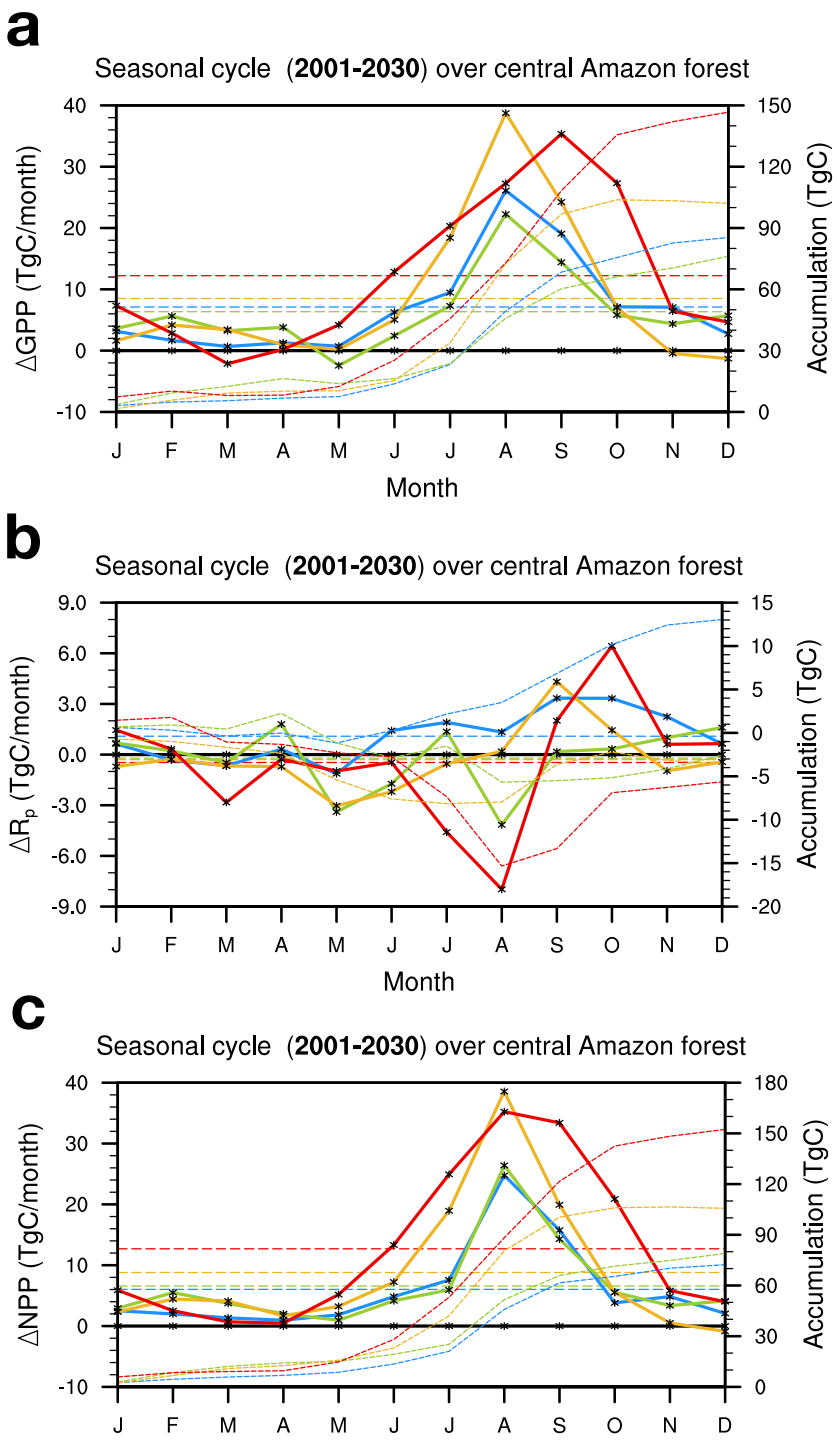

Figure S9: Mean seasonal cycle of GPP anomalies (a), Plant Respiration, R_p, anomalies (b) and NPP anomalies (c) for the varying BBA emission scenarios (see text, section 2.2) averaged over the Amazon basin defined by the coordinates EQ-15°S / 70°W-53°W. Differences are calculated with regards to experiment BBAx0 and represented by the plain curves (left axis). The short-dash curves correspond to the accumulated anomalies (right y-axis). Note the reduced scales on the y-axis on b).

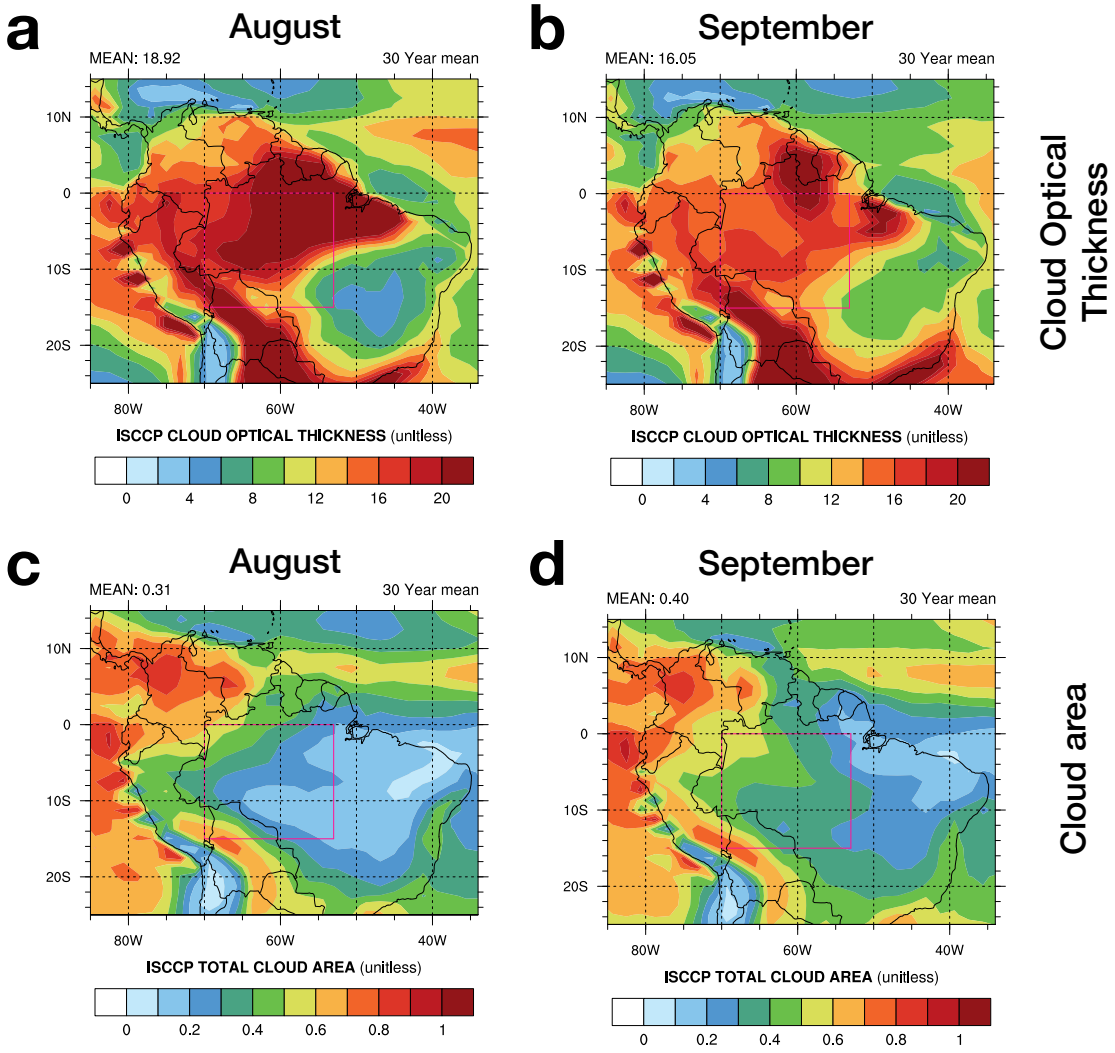

Figure S10: Showing the 30-year mean from the BBAx1 simulation of the in-cloud cloud optical thickness (a,b) and the total cloud fraction (c,d) for August (left) and September (right).

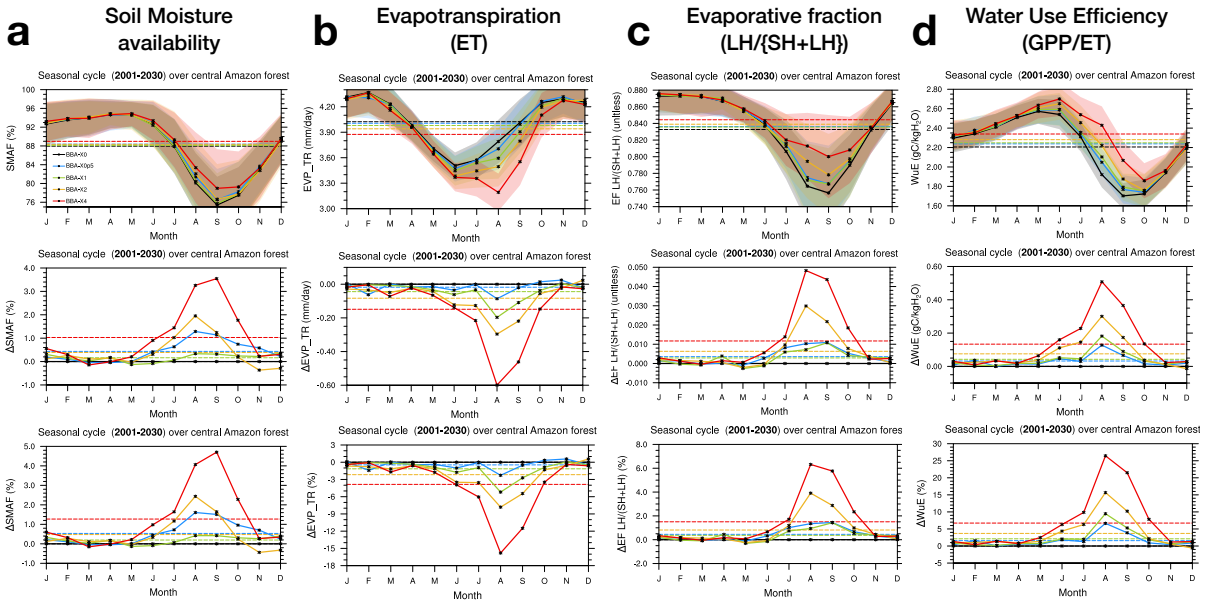

Figure S11: Showing changes in a) Soil moisture availability, b) vegetation evapotranspiration, c) evaporative fraction and d) Water Use Efficiency for the varying BBA emissions scenarios averaged over the domain of analysis defined by the coordinates EQ-15°S / 70°W-53°W (see text).

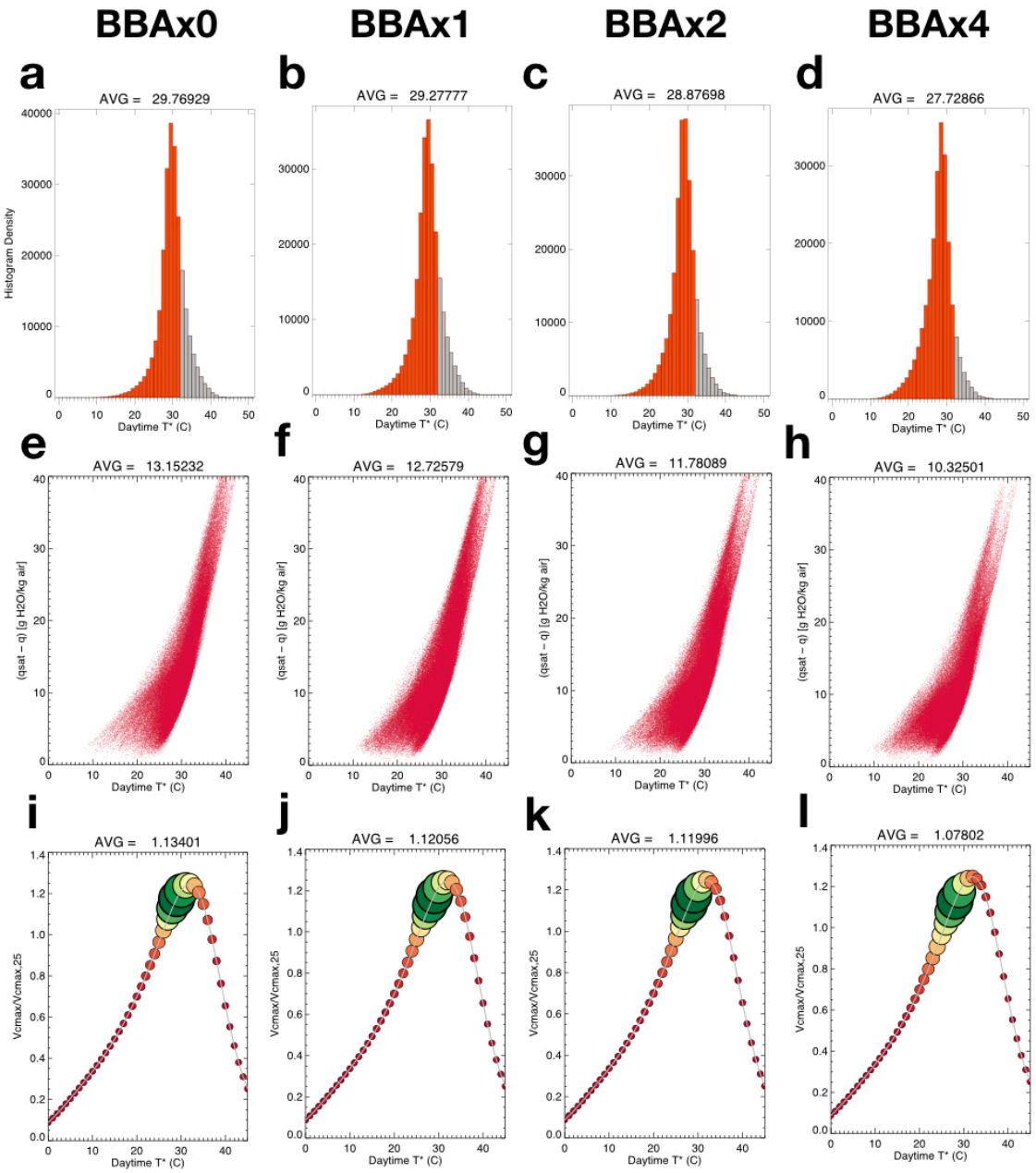

Figure S12: Canopy temperature (first row), Vapour Pressure Deficit (VPD, second row) and Rate of carboxylation of the Rubisco enzyme ($V_{c,max}$) normalised by the maximum rate at 25°C ($V_{c,max,25}$, third row) for the reference simulation (BBAx0, a, e, i) and for the simulations that include BBA emissions (respectively, BBAx1, b,f,j; BBAx2, c,g,k and BBAx4, d,h,l). VPD and $V_{c,max}$ are calculated using the Collatz et al. (1991, 1992) C3 model and assuming the plant functional type traits of broadleaf trees from HadGEM2-ES (Clark et al., 2011). Calculations are done 'a posteriori' (i.e. offline) using the radiation and the meteorological variables derived from the 3h history of HadGEM2-ES instantaneous outputs of the first 8 years of simulation which are sampled over the domain of analysis during daytime when the surface total radiation is superior to 100 W/m^2. As $V_{c,max}$ is solely a function of leaf temperature, we have represented the theoretical curve (in grey). The size of the circles in the bottom plots represent the frequency of occurrence of a given temperature value in the dataset sampled over the domain of analysis defined by the coordinates EQ-15°S / 70°W-53°W.